Protein ingredient quality of infant formulas impacts their structure and kinetics of proteolysis under in vitro dynamic digestion

Lucile Chauvet, Olivia Ménard, Yann Le Gouar, Gwénaële Henry, Julien Jardin, Marie Hennetier, Thomas Croguennec, Marieke van Audenhaege, Didier Dupont, Marion Lemaire, et al.

Protein ingredient quality of infant formulas impacts their structure and kinetics of proteolysis under *in vitro* dynamic digestion

Lucile Chauvet[abc], Olivia Ménard[a], Yann Le Gouar[a], Gwénaële Henry[a], Julien Jardin[a], Marie Hennetier[d], Thomas Croguennec[a], Marieke Van Audenhaege[c], Didier Dupont[a], Marion Lemaire[c], Isabelle Le Huërou-Luron[b], Amélie Deglaire[a*]

[a] INRAE, Institut Agro, STLO, 35042 Rennes France ; [b] Institut NuMeCan, INRAE, INSERM, Univ Rennes, Saint Gilles ; [c] SODIAAL International, Centre Recherche & Innovation, Rennes; [d] Université de Toulouse, Institut National Polytechnique de Toulouse – Ecole d'ingénieur de Purpan, Département Sciences Agronomique et Agroalimentaire, Toulouse.

* Corresponding author: amelie.deglaire@agrocampus-ouest.fr, Amélie Deglaire, Département Productions Animales, AgroAlimentaire et Nutrition, UMR STLO, INRAE, 65 rue de Saint Brieuc, CS 84215, 35042 Rennes Cedex, France

[1] IFs: Infant formulas; [2] WPs: Whey proteins; [3] GMP: Glycomacropeptide; [4] BLG: β-lactoglobulin; [5] ALA: α-lactalbumin; [6] AA: Amino acid; [7] AF_4: Asymmetric flow-field flow fractionation; [8] TEM: Transmission electronic microscopy; [9] SDS-PAGE: Sodium dodecyl-sulfate polyacrylamide gel electrophoresis ; [10] CLSM: Confocal laser scanning microscopy ; [11] TN: Total nitrogen; [12] NPN: Non-protein nitrogen; [13] NCN: Non-casein nitrogen; [14] OPA: o-phtalaldehyde; [15] DH : Degree of hydrolysis; [16] BSA: Bovine serum albumin; [17] LF: lactoferrin; [18] GLC1: Glycosylation-dependent cell adhesion molecule 1; [19] OSTP: osteopontin; [20] ACE: Angiotensin I-converting enzymes; [21] CaMPDE: Calmodulin-dependent cyclic nucleotide phopshodiesterase

Declaration of interests:

This work was supported by SODIAAL International, a French dairy cooperative, as a CIFRE (Agreement of Training through Research) PhD. Lucile CHAUVET, Marieke Van Audenhaege and Marion Lemaire are employed by SODIAAL International. Other authors declare no conflict of interests.

Abstract:

Infant formula (IF) is a complex matrix requiring numerous ingredients and processing steps. The objective was to understand how the quality of protein ingredients impacts IF structure and, in turn, their kinetics of digestion. Four powdered IFs (A/B/C/D), based on commercial whey protein (WP) ingredients, with different protein denaturation levels and composition (A/B/C), and on caseins with different supramolecular organisations (C/D), were produced at a semi-industrial level after homogenization and spray-drying. Once reconstituted in water (13 %, wt/wt), the IF microstructure was analysed with asymmetrical flow field-flow fractionation coupled with multi-angle light scattering and differential refractometer, transmission electron microscopy and electrophoresis. The rehydrated IFs were subjected to simulated infant *in vitro* dynamic digestion (DIDGI®). Digesta were regularly sampled to follow structural changes (confocal microscopy, laser-light scattering) and proteolysis (OPA, SDS-PAGE, LC-MS/MS, cation-exchange chromatography). Before digestion, different microstructures were observed among IFs. IF-A, characterized by more denatured WPs, presented star-shaped mixed aggregates, with protein aggregates bounded to casein micelles, themselves adsorbed at the fat droplet interface. Non-micellar caseins, brought by non-micellar casein powder (IF-D) underwent rearrangement and aggregation at the interface of flocculated fat droplets, leading to a largely different microstructure of IF emulsion, with large aggregates of lipids and proteins. During digestion, IF-A more digested (degree of proteolysis +16%) at 180 min of intestinal phase than IF-C/D. The modification of the supramolecular organisation of caseins implied different kinetics of peptide release derived from caseins during the gastric phase (more abundant at G80 for IF-D). Bioactive peptide release kinetics were also different during digestion with IF-C presenting a maximal abundance for a large proportion of them. Overall, the present study highlights the importance of the structure and composition of the protein ingredients (WPs and caseins) selected for IF formulation on the final IF structure and, in turn, on proteolysis. Whether it has some physiological consequences remains to be investigated.

Keywords: Nutrition, infant formula, protein ingredient, casein, whey, microstructure, *in vitro* digestion, proteolysis

1. Introduction

Despite the WHO recommendations of an exclusive breastfeeding until 6 months of age, a majority of the worldwide infants under 6 months of age (52 %) receive a human milk substitute (Global UNICEF, 2022). Infant formulas (IFs) are the most adequate human milk substitute that is closely regulated and that covers the nutritional needs of the 0- to 6-month-old infants, i.e. until the introduction of appropriate complementary feeding (European Union, 2016). During the last decades, IF composition has been optimized to mimic as closely as possible human milk composition. However, differences in terms of composition and structure still exist and can partly explain the different health effects of IF vs. human milk still observed on the short- and long-term (Lemaire et al., 2018). While many studies have focused on the quality of the lipid fraction in IFs and its impact on digestion and physiology (Bourlieu et al., 2015; Gallier et al., 2015; Le Huërou-Luron et al., 2018; Lemaire, 2018; Oosting et al., 2012), the interest towards the composition and structure of protein fraction of IFs is more recent (Halabi et al., 2022; Huppertz et Lambers, 2020).

IFs are mainly obtained by combining powder skimmed bovine milk with whey proteins (WPs) in order to mimic the casein: whey protein ratio of mature human milk (40:60). These dairy ingredients receive several heat treatments during their own production process before being further processed during IF manufacturing and combined with other ingredients (fat, lactose, minerals and vitamins). WP ingredients can be obtained *via* different processing routes leading to difference in composition and structure of the nitrogenous fraction. The most commonly used WP ingredients in IF are from cheese whey, and less frequently from ideal whey obtained after skimmed milk microfiltration. Cheese whey contains a glycomacropeptide (GMP), a C-terminal hydrophilic peptide released after chymosin cleavage of the Phe105-Met106 bond of κ-casein during cheese manufacturing. GMP is the third most abundant nitrogenous compound in cheese whey after β-lactoglobulin (BLG) and α-lactalbumin (ALA) with typical proportions between 20 to 25 % of total proteins (Thomä-Worringer et al., 2006). GMP has an unbalanced amino acid (AA) profile with only 47 % of essential AAs including no aromatic AA (Phe, Tyr, Trp) and no cysteine (Cys), thus limiting their amount in IFs (Neelima et al., 2013), while purified WPs contain 59 % of essentials AA (Debry, 2001). The processing routes of WP ingredients depend on the desired end-product (lactoserum, concentrate, isolate) and producing companies (nature and order of processing steps, number and intensity of heat treatments). WP processing routes have an impact on WP composition and structure, which was demonstrated to modify digestion kinetics of dairy matrices (van Lieshout et al., 2019) and fat-free model IFs (Halabi et al., 2022). Therefore, the impact of the WP ingredient quality on IF complex structure and in turn on IF digestion should be investigated. Regarding caseins, they are naturally associated into micelles that are supramolecular structures composed of thousands of casein monomers and are rich in calcium and inorganic phosphate. The release of micellar calcium phosphate from the micelles modifies the supramolecular structure of the casein micelles and increases the fraction of non-micellar caseins. This change in the supramolecular organisation (micellar or non-micellar) of caseins can impact the gastric digestion and emptying kinetics (Dupont et al., 2010; Wang et al., 2018). Recently, it was reported that non-micellar caseins presented a lower level of gastric coagulation, with smaller and weaker curd particles potentially increasing their gastric emptying pace (Huppertz et Lambers, 2020). This could be a way to better mimic human milk, which has smaller casein micelles (30 - 70 nm) than bovine milk (130 - 160 nm), potentially partly explaining the faster gastric emptying for human milk than for IF (Billeaud et al., 1990; Cavell, 1981; Ewer et al., 1994; Van Den Driessche et al., 1999).

The present work aimed to investigate the effects of the quality of different commercial protein ingredients (WP and caseins) on IF structure and in turn on IF digestion kinetics. Four powdered IFs were produced with commercial protein ingredients, presenting different protein quality, following the same processing route at a semi-industrial scale. The influence of WP ingredient structure and composition and of casein supramolecular organisation on IF structure was investigated at different scales. The structure of IF was analysed using the asymmetrical flow field-flow fractionation (AF_4-

MALS-dRI) coupled with multi-angle light scattering and differential refractometer, transmission electron microscopy and confocal laser scanning microscopy. IF digestion kinetics (structure and proteolysis) were investigated using an *in vitro* dynamic model at a 4-week-old infant stage.

2. Material and methods

2.1. Infant milk formula ingredients and processing

Standard skimmed milk powder and casein concentrate powder were provided by SODIAAL (Nutribio, Doullens, France). Skimmed milk powder was characterized by a crude protein content of 35.5 % with a casein:whey proteins ratio of 80:20 and casein concentrate powder milk by a crude protein content of 60 % with a casein:whey protein ratio of 90:10. A non-micellar casein ingredient was also provided by SODIAAL (Eurosérum, Port-sur-Saône, France) with a crude protein content of 26 % and a casein:whey protein ratio of 65:35. Three commercial WP powders were purchased from dairy companies. Their main characteristics are presented in Table 1 and their global processing route is given in Figure 1. Lactose, minerals, vitamins were provided by SODIAAL (Nutribio, Doullens, France). Non-dairy fat (a blend of palm, sunflower, oleic sunflower and rapeseed oils with lecithin as emulsifier and ascorbyl palmitate and a blend of tocopherols as anti-oxidants) was purchased at SODECO (Château-Renard, France).

Four powdered IFs (A, B, C, D) were formulated following the European regulation (EU, 2016/127) in order to have similar amino nitrogen and mineral content. IFs-A, -B and -C contained skimmed milk powder as a source of caseins (micellar form), while IF-D contained a mix of non-micellar caseins (75 % of total caseins) and casein concentrate powder (micellar caseins representing 25 % of total caseins). Regarding whey proteins, IF-A was based on the demineralized cheese whey powder, IF-B on the demineralized cheese whey protein concentrate powder and IFs-C and -D on the demineralized ideal whey powder (Table 1). Different forms of minerals (Supplementary data 1) were used among IFs in order to have the same concentration of each mineral across IFs. Formulation specificities were given in Supplementary data 2.

All four IF powders (~ 200 kg per IF) were produced in a similar manner at a semi-industrial scale at Bionov (Rennes, France). Protein ingredients, minerals, choline and vitamins were rehydrated at 42 % (wt/wt) of dry matter and mixed at 50 °C under stirring. KOH (40 % v/v) was then added to reach a pH of 6.1 ± 0.1. The fat blend was stirred at 55 °C before being homogenized in line with the wet mix (50 °C, 80/20 bar). Homogenised mix was pasteurized (72 °C, 2 min) and then spray-dried using a semi-industrial-scale 2-stage spray-dryer (Niro Atomizer, GEA-PE, Saint Quentin en Yvelines, France) at Bionov (Rennes, France), for which maximum theoretical evaporation capacity is approximately 90 kg / h. The inlet air temperature was set at 206 ± 2 °C and the outlet air temperature was set at 90 ± 2 °C. Flow rate was 110 L / h and the major airflow rate was 2260 ± 50 kg / h. Powdered IFs were then stored in big bags before addition of pro-oxidants minerals and docosahexaenoic acid and final packaging in metal tins under modified atmosphere.

2.2. *In vitro* dynamic digestion material and protocol

Materials were all standard analytical grade. Chemicals, bile, enzymes and their respective inhibitors were purchased from Sigma-Aldrich (St Quentin Fallavier, France) except for rabbit gastric extract purchased from Lipolytech (Marseille, France). Enzymes' activities and bile activity were determined using the method described by Brodkorb et al. (2019).

In vitro gastrointestinal dynamic digestion of the four rehydrated IFs (13 g of powder added in 87 g of warm water, 37 °C) was done using the bi-compartmental system called DIDGI® (Ménard et al., 2015). This *in vitro* dynamic digestion system was configured as described by Nebbia et al. (2020) with

modifications in order to simulate the digestive conditions of a term four-week old infant born. The gastric and intestinal emptying followed an exponential equation, as described previously (Elashoff et al., 1982). For the gastric phase, a gastric emptying half-time ($T_{1/2}$) of 78 min and a β coefficient of 1.8 were used and for the intestinal phase a $T_{1/2}$ of 200 min and a β of 2.2 were applied. Gastric enzymes consisted of pepsin and rabbit gastric extract (268 U of pepsin and 19 U of lipase per ml of gastric content), intestinal enzymes covered by pancreatin (16 U of trypsin / mL of intestinal content) and bile to provide 3.1 mmol of bile salts /ml of intestinal content. Total digestion duration was 180 minutes. For each IF, the digestion was performed in triplicate (n = 3).

Samples were collected before (undigested IFs) and during digestion in both gastric and intestinal compartments at 20, 40, 80 ,120 and 180 min (G20, G40, G80, G120 and G180 for gastric phase samples, and I20, I40, I80, I120 and I180 for intestinal phase samples). Proteases and lipases were inhibited as described in Nebbia et al. (2020). Samples were stored at -20 °C, except for the structural analysis performed on fresh samples.

2.3. Structural characterisation

2.3.1. Asymmetric flow-field flow fractionation (AF_4-MALS-dRi)

AF_4 coupled with multi-angle light scattering and differentials refractometer was used to study entities in IFs (1.45 % of proteins) diluted (2-fold) in an eluant (50 mM NaCl and 5 mM $CaCl_2$ in milliQ water at pH 7.6 filtered through 0.1 µm). AF_4 analyses were done using a Thermo Scientific Dionex UltiMate3000 HPLC System with pump, autosampler and UV detector (set at 280 nm). The pump was coupled with the Eclipse AF_4 (Wyatt Technology). A multi-detection system including an 8-angle Dawn8+ MALS detector and an Optilab TrEX dRI (Wyatt Technology) was coupled with the AF_4 system. Chromeleon 6.0 software was used to control the autosampler, pump and Eclipse flows. Injections of samples (2 µl) was controlled with an Agilent 1260 Autosampler (Agilent technologies, Waldbronn, Germany). Elution and focus periods, channel, spacer, membrane and data analysis were as described in Halabi (2020).

2.3.2. Transmission Electronic Microscopy (TEM)

Each IF was analysed by TEM as described in Halabi (2020) excepted that IFs were rehydrated at 3 % (wt/wt) of true proteins. Imaging was carried out with a JEM-1400 Transmission Electron Microscope (JEOL CO. Ltd, Tokyo, Japan) operating at 120 kV accelerating voltage. Images were recorded with a Gatan SC200 Orius® CCD camera at 50 000 magnification and set up with the imaging software Gatan Digital Micrograph™ (Gatan, Pleasanton, USA). Images were acquired on at least two different regions of each thin layer cut out of at least two different blocks.

2.3.3. Sodium docedyl-sulfate polyacrylamide gel electrophoresis (SDS-PAGE)

These analyses aimed to investigate the supramolecular organisation of caseins after IF processing. IFs were rehydrated in milliQ-water at 1.45 % of proteins. SDS-PAGE was performed on rehydrated IFs after different physical separations: as is, after skimming (15 000 g, 1 h) or after skimming and ultracentrifugation to discard micellar caseins (Sorvall Discovery™ 90 SE Ultracentrifuge, Hitachi Ltd, Tokyo, Japan). Two different rotation speeds (100 000 or 50 000 g, 1 h, 25 °C) were used. SDS-PAGE was performed with a loading of 6 µg of protein in each well. Band densitometry was conducted using ImageQuantTL software (GE Healthcare Europe GbmH, Velizy-Villacoublay, France) for a semi-quantitative analysis of the proportion of IF proteins at the interface of the fat droplet or of the soluble caseins.

2.3.4. Particle size distribution

Particle size distribution of reconstituted IFs and of the digesta at 20, 40, 80 and 120 min of gastric phase were determined using laser light scattering as described in Halabi et al. (2020) (Malvern Mastersizer 2000, Malvern Instrument Ltd., Worcestershire, UK).

2.3.5. Confocal laser scanning microscopy (CLSM)

The microstructure of IFs and digesta at 20, 40, 80 and 120 min in the gastric compartment were observed by CLSM as described in Halabi et al. (2022) adding the use of RedNileFast to label lipids (18 µl of 0.1 % (w/v) Nile Red 1,2-propanediol solution). Observation was performed using 488 and 633 nm excitation wavelengths in sequential beam fluorescent mode, for fat and protein detection, respectively, Red Nile and Fast Green were detected using a GaasP between 550 and 590 nm and a PMT between 635 and 735 nm, respectively. Confocal analysis was performed for each IF on two *in vitro* digestion (n = 2).

2.4. Biochemical analysis

2.4.1. Nitrogen content

Total nitrogen (TN), non-protein nitrogen (NPN) obtained after sample precipitation by trichloroacetic acid (12 %, wt/vol) and non-casein nitrogen (NCN) obtained after sample precipitation at pH 4.6, were determined by the Kjeldahl method (IDF, 2014), with a nitrogen to protein conversion factor of 6.38. The NCN fraction contains all the nitrogen compounds except caseins and irreversibly denatured and aggregated WPs that precipitate at pH 4.6. Among the nitrogen compounds soluble at pH 4.6 are native, glycated, and reversibly denatured or aggregated WPs, as well as GMP, peptone proteoses, and the NPN fraction.

Overall protein denaturation level of IF was determined according to Equation 1:

$$Denaturation\ level\ (\%) = 100 - \left(\frac{(NCN - NPN)}{(TN - NPN) \times proportion\ of\ whey\ proteins} \times 100\right) \qquad (1)$$

$$= 100 - \left(\frac{Soluble\ proteins\ at\ pH\ 4.6}{Total\ whey\ proteins} \times 100\right)$$

2.4.2. Primary amine content

Undigested IFs and gastric and intestinal digesta (20, 40, 80, 120 and 180 min) had their primary amino group quantified using the *o*-phtalaldehyde (OPA) method (Church et al., 1983; Nielsen et al., 2001). Modification was made by diluting the soluble fraction of digesta in 50 mM sodium tetraborate buffer. Each sample was analysed in triplicate (n = 3). The degree of hydrolysis (DH) was calculated as following after considering the dilution by gastrointestinal secretions and emptying (Equation 2):

$[NH_2]_{digesta}$ was the primary amine content in the gastric or intestinal digesta (mg / L of IF), $[NH_2]_{enzymes}$ set at 0 for the gastric phase and corresponding to the primary amine content in the undigested

$$DH\ (\%) = \frac{[NH_2]_{digesta} - [NH_2]_{enzymes} - [NH_2]_{undigested\ IF}}{[NH_2]_{total\ undigested\ IF} - [NH_2]_{undigested\ IF}} \times 100 \qquad (2)$$

pancreatin for the intestinal phase (mg / L of IF), $[NH_2]_{undigested\ IF}$ the primary amine content in the undigested IF (mg / L of IF) and $[NH_2]_{total\ undigested\ IF}$ the total content of primary amines in IF after complete acid hydrolysis (6 N HCl at 110 °C during 24 h) (mg / L of IF).

2.4.3. Semi-quantification of protein hydrolysis

Undigested IF and digesta were analysed by SDS-PAGE, such as described in 0, except that the protein amounts loaded into the well were determined based on a loading equivalent to 5 or 30 µg of proteins from the undigested IFs in the gastric or intestinal phase, respectively. Pepsin and pancreatin solutions were also loaded on the gels in similar amounts to those of the gastric and intestinal samples. The proportion of residual intact proteins in the digesta, resulting from hydrolysis and dilution by digestive secretions, was calculated at each time of digestion following the Equation 3:

$$Intact\ residual\ protein\ (\%) = \frac{Band\ intensity_{digested\ IF}}{Band\ intensity_{undigested\ IF}} \times 100 \qquad (3)$$

2.4.4. Peptide identification and quantification

Digesta were analysed by mass spectrometry with a nano-RSLC DIonex U3000 system fitted to a Q-Exactive mass spectrometer (Thermo Scientific, Sans Jose, USA) equipped with a nanoelectrospray ion source, such as previously described (Halabi et al., 2022). Peptides were identified from the MS/MS spectra using the X!TandemPipeline software (Langella et al., 2017) and then quantified by label-free MS using MassChroQ software (Valot et al., 2011). When a peptide was measured with several charge states, all ion intensities were summed. For peptide identification, a homemade protein database composed of major bovine milk proteins (131 proteins) was used. Bioactive peptides were identified using an exact matching of the sequence with the BIOPEP database (Minkiewicz et al., 2008), accessed in May 2022.

2.4.5. Amino acid quantification and bioaccessibility

Total and free AA contents were measured in duplicate (n = 2) freshly reconstituted IFs. The total AA contents were determined after a 24 h acid hydrolysis at 110 °C in 6 N hydrochloric acid. The sulfur-containing AAs, Cys, and methionine (Met), were measured as methionine sulphone and cysteic acid after performic acid oxidation. The free AA contents, except Trp were determined after deproteinization of the samples with sulfosalicylic acid at a final concentration of 2.5 %. Free AA contents were also quantified during *in vitro* dynamic digestion (I20, I40, I80, I120, I180) and in pancreatin and bile solution. Injections of total and free AAs were done on the cation exchange column of Biochrom 30 automatic AA analyser (Biochrom Ltd, Cambridge, UK) with post-column derivatization with ninhydrin (EZ Nin Reagent™, Biochrom Ltd, Cambridge, UK). Ninhydrine derivative of all AAs was detected at 570 nm (except proline at 440 nm). Trp was quantified individually in duplicate (n = 2) freshly reconstituted IFs using the method described in Charton et al. (2022).

AA bioaccessibility was then calculated according to the following calculation (Equation 4):

$$AA\ bioaccessibility\ (\%) = \frac{Free\ AA_{digested\ IF} - Free\ AA_{enzymes}}{(Total\ AA_{undigested\ IF} - Free\ AA_{undigested\ IF})} \times 100 \qquad (4)$$

Free $AA_{\text{digested IF}}$ was the content of free AA in the digesta (g / kg IF), free $AA_{\text{undigested IF}}$ was the content of free AA measured in the IF before digestion (g / kg IF) and total $AA_{\text{undigested IF}}$ was the content of total AA within IFs (g / kg IF).

2.4.6. Statistical analysis

Statistical analyses were conducted using R software (version 4.2.1). Hydrolysis degree, proportion of intact residual proteins and AA bioaccessibility were analysed using a mixed linear model (lmerTest

package) with meal and time as fixed factors and digestion replicates as random factor. Residual normality and variance homogeneity were tested for each factor and all variables using Kolmogorov-Smirnov test (nortest package) and Levene test (lawstat package), respectively. Differences were considered as statistically significant when p-value was strictly below 0.05. Pairwise multiple comparisons of the means were carried out using Tukey's test (lsmeans package).

Only peptides identified in at least two digestion replicates among the three digestion replicates per IF were kept. Peptides unidentified in only one digestion replicate of IFs had their abundance set to 0.

The peptide abundances were summed by protein, log10-transformed (log10(abundance+1) and the maximum abundance was set to 1. Hierarchical clustering was then performed, based on the minimum within-cluster variance Ward's agglomeration (hclust function; stats package). The number of clusters was determined thanks to the bar heights at one of the most marked jumps. The heatmap and its dendrogram were then displayed (heatmap.2 function; stats package).

3. Results and discussion

3.1. Whey protein denaturation levels in the IFs

Moderate differences were observed regarding crude protein contents among IFs (Table 2), with a crude protein content of IF-B being 9 % lower than that in other IFs. The difference in NPN content observed among IFs (Table 2) mostly reflected the differences observed among WP ingredients (Table 1). A higher concentration of Trp was observed in IF-C and IF-D (+.22.%) than in IF-A and -B, due to the ideal whey used in IFs-C and -D containing a higher content of ALA and BLG and no GMP.

WPs provided by demineralized cheese lactoserum (IF-A) had the most denatured WPs out of the three WP ingredients, resulting in the highest WP denaturation level for IF-A (44.3 ± 0.01.%), as presented in Table 2. The denaturation levels of IF-C and IF-D were respectively 30 and 34 % lower than that of IF-A, in agreement with the lower WP denaturation in the ideal whey. The denaturation level of IF-B was intermediate with a value of 35.9 %, while BLG and ALA within the WP ingredient were not observed as denatured (Table 1). This high increase of protein denaturation between the ingredients and the IF can be explained by the higher heat sensitivity of native WPs while pre-heat treatment has been reported to have a preventive effect on further protein denaturation/aggregation during subsequent heat treatment (Joyce et al., 2017).

The WP denaturation levels in IFs (Table 2) were lower than those previously reported in commercial IFs (65 ± 11 % according to Yu et al., 2021). This is likely be due to the absence of the vacuum evaporation step within the present IF processing route, as this unit operation, when coupled to a standard high heat treatment (90 °C, 2 - 3 s), can increase by 25 percentage points the denaturation level (Yu et al., 2021).

3.2. Multi-scale structural characterisations of the IFs

IFs-A, -B and -C presented similar particle size distribution (Figure 2.A) before digestion with a main modal diameter of 0.63 ± 0.03 µm, while IF-D had an additional peak at a modal value of 7.2 ± 0.5 µm. This latter peak corresponded to aggregates of fat droplets and casein micelles as dissociated by addition of SDS and EDTA, respectively (data not shown). This was confirmed by CLSM and TEM images (Figure 2.B), where IF-D presented some insoluble micronic protein particles and larger aggregates of fat droplets covered by denser, smoother and more numerous round casein structures. IF-A showed different protein structures around fat droplets, with a proteic star shape surrounding them (Figure 2.B, CLSM images). This is likely due to the heat-induced WP aggregates bound to the κ-casein of the casein micelles, as seen in Kalab et al. (1983) and Halabi (2020), themselves adsorbed at

the fat droplet interface (Figure 2.B). No difference in shape was observed between IF-B and IF-C with casein micelles visible at the interface of the lipid droplets (Figure 2.B, CLSM and TEM images).

Fractograms of IFs-A, -B and -C (Figure 2.C), as obtained by AF_4-MALS-dRI, showed three distinct populations of individual WPs between 9 to 13 min, intermediate protein structures (casein micelles, WPs aggregates, casein and WPs small aggregates) between 13 to 22 min and particles formed by the interaction of proteins and lipids between 22 to 30 min. The fractogram of IF-D could not be obtained due to the presence of some insoluble particles and a partial adhesion of residual aggregates onto the membrane in the channel, thus resulting in the system clogging. The first peak identified in the fractogram (individual WPs) was smaller but wider for IF-A than for IFs-B and -C (Figure 2.C), which could be partly explained by the higher level of glycation of the WP ingredients (Table 1) leading to an increase of the molecular weight and thus delayed elution time. A higher gyration radius (R_g) of particles was determined for IF-A than for IFs-B and -C (Figure 2.C), which likely corresponds to the WP appendages at the surface of the casein micelles themselves adsorbed onto the fat droplets (Figure 2.B). As the refractive index of the protein and lipid mix is not known, the shape factor could not be determined to confirm these observations.

Thanks to SDS-PAGE analyses, when comparing the skimmed IFs before and after ultracentrifugation, the soluble caseins were estimated to be in the same proportion in all the IFs (51 ± 6 %, $p > 0.05$), indicating that the non-micellar casein ingredient used for IF-D underwent some rearrangement during processing. At an intermediate ultracentrifugation scale (50 000 *g*), the soluble casein proportion was even lower for IF-D (15 ± 7 %) than for IFs-A, -B and -C (respectively 27 ± 1 %, 29 ± 3 % and 29 ± 1 %), indicating that part of caseins in IF-D were included into bigger structures than in other IFs. This is likely due to the addition of tricalcium phosphate and other forms of calcium (calcium chloride, calcium carbonate) during IF processing, which must have favoured casein reassociation in IF-D (Swaisgood, 1992). In particular, the addition of calcium chloride to a caseinate solution, prior to the addition of fats and prior to homogenisation, such as for IF-D, has been reported to cause an increase in the average droplet size and the droplet surface protein concentration (Srinivasan et al., 1996; Ye et Singh, 2001). Whether the addition of certain form of calcium after homogenisation or after spray-drying during dry-mixing with DHA and pro-oxidant minerals could reduce droplet flocculation and casein aggregation is not known. Further work is still needed to better understand the impact of calcium on caseins, especially caseinate, during and after the processing of a complex matrix such as IFs.

In overall, the multiscale structural analysis showed that IF-A had a peculiar structure with denatured WPs aggregated at the interface of casein micelles, the latter being adsorbed at the surface of fat droplets, as schematically represented in Figure 2.D. IFs-B and -C appeared to have a similar microstructure with a mixture of both native and denatured/aggregated WPs in the soluble phase, and with caseins adsorbed at the surface of fat droplets. Regarding IF-D, large aggregates of fat droplets, denatured/aggregated WPs and caseins were observed (Figure 2.D).

3.3. *In vitro* dynamic digestion

3.3.1. Structural changes during gastric digestion

Figure 3 shows the particle size distribution (Figure 3.A) and the microstructure as observed by CLSM (Figure 3.B) of the IFs at 40, 80 and 120 min of gastric digestion (G40, G80, G120). At G40 (pH 5.6), aggregates were formed for all IFs (Figure 3). IF acidification to pH 5.6 did not modify their particle size distribution (Figure 3.A). Such aggregation is thus likely due to the pepsinolysis of κ-casein causing rapid aggregation of para-casein micelles and subsequently of the fat droplets surrounded by casein micelles. Aggregate sizes were different among IFs, with larger microstructures for IFs-A and -B than IFs-C and -D (Table 3). Star-shaped structures observed in undigested IF-A were no more

visible (Figure 3.B). IF-C showed a denser distribution of small compact aggregates, while IF-D had smaller microstructures than any other IFs (Figure 3), probably linked to the modified casein structures likely having a different susceptibility to pepsinolysis as micellar caseins. The differences observed between IF-B and IF-C could be explained by their different protein profiles. Indeed, BLG and ALA accounted for 50 % of the true protein in IF-C while they only accounted for 43 % in IF-B, because of the presence of GMP. Although the structural analysis before digestion did not reveal any difference, it is possible that the composition of the interface of casein micelles was not the same and, in IF-B, favoured the access of pepsin to κ-casein leading more rapidly to casein aggregation compared to IF-C.

At G80 (pH 4.8), the particle size increased for all IFs (Table 3 and Figure 3.A), with a significantly higher modal diameter for IF-A than for the other IF-s (37.3 ± 3.0 µm *vs* 27.7 ± 1.4 µm). This increase in size was the result of pH acidification and pepsinolysis, the latter allowing a particle size reduction as compared to the sole acidic aggregation (Figure 3.A). At pH 4.8, coagulation occurred for casein micelles coated with denatured WPs (IF-A) and, to a lower extent, for native micelles (IFs-B and -C) as the digestive pH was close to their isoelectric points (pI), being respectively 5.1 and 4.7 (Guyomarc'h et al., 2003). In addition, the net charge of main WPs (BLG and ALA, pI 5.1-5.2) decreased, favouring their aggregation and/or interaction between WPs and uncharged lipids, as seen in Le Roux et al. (2020). Similar tendencies among IFs were observed at G120.

3.3.2. Proteolysis degree

The degree of proteolysis of IFs increased progressively over time ($p < 0.001$) during the gastric and intestinal phases (Figure 4.A). The gastric proteolysis was low, such as previously observed (Abrahamse et al., 2022; Halabi et al., 2022; Le Roux et al., 2020), due to a combined effect of a low pepsin activity and a high gastric pH (6.8 to 4.2 before 120 min). During the intestinal phase, IF proteolysis rapidly increased over the first 40 min of digestion (x 2 in 20 min, Figure 4.A) and then followed a linear increase. Differences between IFs were only observed at 180 min of both gastric and intestinal phases, with IF-A being significantly more hydrolysed than IF-C in the gastric phase (+18%) and IF-D in both phases (+ 16%). This could be linked to the structure of IF-A, with the WP aggregates bounded to casein micelles adsorbed on the fat droplets, thus potentially increasing the enzyme accessibility and leading to a higher proteolysis, such as demonstrated for BLG being more hydrolysed when adsorbed at the interface of fat droplets than when in the soluble phase (Macierzanka et al., 2009).

3.3.3. Residual intact proteins in the gastric phase

The kinetics of disappearance of intact BLG, ALA and caseins during the gastric phase are presented in Figure 4.B, concomitantly with the proportion of IF in the digesta (dotted line) in order to differentiate the dilution of the dietary proteins by the digestive fluids from their proteolysis. Although differences of structures and hydrolysis degree were shown between IFs, no significant difference was observed in the kinetics of gastric disappearance of the intact proteins (BLG, ALA, caseins) between IFs. However, a tendency (p-value = 0.08) was observed for caseins, which tended to be more hydrolysed in IF-A than in IF-D (respectively 64.6 ± 10 % and 82.1 ± 8 % of residual intact caseins) at G40 (Figure 4.B). This could be in line with the larger microstructure observed at G40 for IF-A than for IF-D, as well as to the neoformed denser casein supramolecular organisation in IF-D. Casein hydrolysis took place between 40 and 80 min of gastric digestion, with virtually no residual intact caseins after that time for all IFs.

In the intestinal phase, no intact protein was observed by SDS-PAGE (data not shown).

3.3.4. Amino acid bioaccessibility

Bioaccessibility of each AA was determined along the intestinal digestion time. Some AA bioaccessibility, such as for Met, Phe and Ile, differed among IFs (Figure 4.C). Met bioaccessibility was significantly higher for IFs-C and -D than for IF-B during the whole intestinal phase and than for IF-A during the latter digestion time (I80 to I180). Similar observations were reported in the literature (de Oliveira et al., 2016) where Met bioaccessibility was greater in raw than in pasteurized human milk. Phe and Ile bioaccessibilities (Figure 4.C) differed among IFs (p-value < 0.001) regardless of the digestion time. IF-A had higher bioaccessibility of Phe than other IFs and of Ile than IFs-C and -D. Differences of AA bioaccessibility could be explained by different residue accessibility to the proteases that depended on the nature and structure of the protein. Moreover, the higher level of Ile in GMP (11% of total AAs) could participate to its higher bioaccessibility, such as in IFs-A and -B based on cheese lactoserum, thus containing GMP. No difference of lysine bioaccessibility was observed among IFs despite the different proportion of blocked lysine among WP ingredients (Table 1).

The present release of free AAs was solely due to the carboxypeptidase, as no brush border enzyme could be included in the model, which has somehow underestimated the overall bioaccessibility and degree of hydrolysis (Picariello et al., 2015).

3.3.5. Kinetics of peptide release

A total of 1061 unique peptide sequences (5 to 50 AAs in length) was identified in the gastric (G80, G180) and intestinal (I20, I40, I80, I180) digesta of the four IFs with 96 % of the sequences common to the four IFs. Eighty-two % of the peptides derived from caseins, with 45.3 % of peptides from β-casein, 16.3 % from α_{s1}-casein, 11.7 % from κ-casein and 8.8 % from α_{s2}-casein. A small fraction of peptides was from WPs (15.3 %) with 12.1 % from BLG, 2.3 % from ALA, 0.5 % from bovine serum albumin (BSA) and 0.4 % from lactoferrin (LF). Finally, 2.3 % of peptides derived from glycosylation-dependent cell adhesion molecule *1* (GLC1) and 0.2 % from osteopontin (OSTP), which are minor proteins naturally present in bovine milk. Our results agreed with the previously reported large proportion of casein-derived peptides, especially β-casein, in IF digestion (Halabi et al., 2022; Hodgkinson et al., 2019; Su et al., 2017; Wada et al., 2017). The low proportion (15.3 %) of WP peptides may be attributed both to the presence of disulphide bonds preventing their identification and to the absence of identification of large (> 50 AAs) or small peptides (< 5 AAs) by the present LC-MS/MS method. The peptide abundancies were summed per protein according to their parent protein. Three clusters were identified (Figure 5.B). Cluster 1 was composed of proteins having peptides detected since the half gastric-emptying time (G80), mainly for caseins, and to a lower extent for GLC1 and LF represented by a limited number of peptides. The peptides deriving from these proteins had a maximum abundance during the gastric phase. Cluster 2 was only composed of BLG from which peptides were detected mainly on the last gastric digestion time (G180) and along the intestinal phase, in line with the BLG resistance in the early gastric digestion time due to a high pH not altering the globular conformation thus hindering pepsin cleavage (Dalgalarrondo et al., 1995). Cluster 3 corresponded to ALA, BSA and OSTP, for which peptides were mostly released at the end of the gastric phase. A few ALA-derived peptides were also detected during the intestinal phase.

Changes in peptide release kinetics were evidenced among IFs (Figure 5.B). IF-D had a higher abundance of casein-derived peptides at G80, which likely result from a greater resistance of caseins to hydrolysis in IF-D, in line with the observations made by SDS-PAGE (Figure 4.B) and attributed to the different initial structure (neoformed denser casein supramolecular organisation). It should be noted that peptides in the region 106-169 from κ-casein was more abundant in IFs-A and -B due to the presence of GMP (cheese whey) in these IFs. Regarding LF, which is a globular protein resistant to digestion, the higher abundance of its peptides observed at the half gastric-emptying time in IFs-A and -B may be, on the contrary, due to a lower digestive resistance of LF thanks to a greater denaturation level (Table 2). However, precaution should be taken as LF-derived peptides represented only 0.3 % of the peptides. IFs-C and -D had more abundant ALA-derived peptides in the

gastric and intestinal phase than IFs-A and -B, as well as BLG-derived peptides in the intestinal phase (Figure 5.C), which may be explained by the higher concentration of ALA and BLG in IFs-C and -D and potentially to more proteolytic resistance of these proteins due to the lower denaturation extent in these two IFs.

3.3.6. Bioactive peptides

Among all the identified peptides, 45 were found to display bioactivity according to the BIOPEP database (Figure 6). The majority (64 %) of these bioactive peptides were identified only during the gastric phase, 18 % were found during both the gastric and intestinal phases and 18 % were specific to the intestinal phase. The bioactive peptides identified during the gastric digestion had more diversified parent proteins than those observed in Halabi et al. (2022), with 27 % of identified peptides deriving from β-casein, 24 % from BLG, 22 % from κ-casein, 16 % from α_{s2}-casein, 8 % from α_{s1}-casein and 3 % from ALA. As observed in Halabi et al. (2022) and Hodgkinson et al. (2019), angiotensin I-converting enzymes (ACE)-inhibitory activity, binding activity and calmodulin-dependent cyclic nucleotide phosphodiesterase (CaMPDE) inhibitor were the main identified bioactivities. During the intestinal phase, the bioactive peptides identified were less abundant and diversified with 44 % coming from β-casein, 38 % from BLG, 12 % from α_{s2}-casein and 6 % from α_{s1}-casein. Bioactivities were mainly ACE inhibitor and binding activities, which play a role in cardiovascular health. ACE-inhibitory peptides might prevent the immaturity-related higher serum ACE activity in early life that is involved in the programmation of cardiovascular disease in adulthood (Wada et Lönnerdal, 2014).

At the end of the gastric phase (G180), IF-C had the highest abundance for 55 % of the bioactive peptides identified, while IF-D, -B and -A had the highest abundance for 24 %, 12 % and 9 % of the bioactive peptides, respectively (Figure 6). At the end of intestinal phase (I180), IF-C also had the highest abundance for 46 % of bioactive peptides identified, while IF-A, B and D had the highest abundance for 31 %, 23 % and only 8 % of the bioactive peptides, respectively (Figure 6). Interestingly, IF-C had the highest abundance for a large proportion of bioactive peptides in both gastric and intestinal phases, in agreement with the lower protein denaturation level in this IF, leading to a higher resistance to hydrolysis.

Each bioactive peptide in the intestinal phase contained between one to four proline residues, explaining their resistance to proteolysis (Halabi et al., 2022). However, whether the inclusion in the digestion model of peptidases from the brush border membrane (Picariello et al., 2015), such as aminopeptidase and dipeptidylaminopeptidase IV that are proline-specific exopeptidases, would have further hydrolysed these bioactive peptides, remains unknown. Besides, the presence of bioactive peptides in the digesta does not necessarily imply that they will pass through the intestinal barrier and exert their bioactivities in the organism although infants have a relatively high intestinal barrier permeability in early life (Lee et al., 2017). Finally, it should be noted that the present method did not allow the detection of peptides smaller than five AAs, which could also present some bioactivity.

4. Conclusion

The present study has demonstrated that the quality (structure and composition) of dairy commercial protein ingredients had a significant impact on the microstructure of IFs and that these differences modulated the proteolysis kinetics as well as the deconstruction of the emulsion in the early gastric phase. WP ingredient with a high denaturation level generated star-shaped microstructures favouring protein hydrolysis. Non-micellar caseins, brought by non-micellar casein powder, led to a largely different microstructure of the IF microstructure, with large aggregates of lipids and proteins. The structure and composition of IFs also impacted the accessibility of the

peptide bonds to enzymes, and the IF with the lower denaturation extent presented the highest abundance of bioactive peptides. Overall, the present work highlights the importance of considering the quality of the protein ingredients when manufacturing IFs. The latter should be as much as possible mimicking HM, including its digestive behaviour; to this end, the comparison of the digestion between HM and IF remains to be investigated. In addition, further *in vivo* investigations are required to evaluate the impact of such IFs on the kinetics of protein digestion and amino acid absorption as well as on the gut physiology.

Acknowledgments:

We would like to thanks Agnès Burel from the Université de Rennes 1, Plateforme de microscopie MRic BIOSIT UMS 3480, 35043 Rennes (France) for the work done on transmission electronic microscopy.

References:

Abrahamse, E., Thomassen, G. G. M., Renes, I. B., Wierenga, P. A., & Hettinga, K. A. (2022). Gastrointestinal Protein Hydrolysis Kinetics: Opportunities for Further Infant Formula Improvement. *Nutrients*, *14*(7), 1512. https://doi.org/10.3390/nu14071512

Billeaud, C., Guillet, J., & Sandler, B. (1990). Gastric emptying in infants with or without gastro-oesophageal reflux according to the type of milk. *European Journal of Clinical Nutrition*, *44*(8), 577–583.

Bourlieu, C., Ménard, O., De La Chevasnerie, A., Sams, L., Rousseau, F., Madec, M.-N., Robert, B., Deglaire, A., Pezennec, S., Bouhallab, S., Carrière, F., & Dupont, D. (2015). The structure of infant formulas impacts their lipolysis, proteolysis and disintegration during in vitro gastric digestion. *Food Chemistry*, *182*, 224–235. https://doi.org/10.1016/j.foodchem.2015.03.001

Brodkorb, A., Egger, L., Alminger, M., Alvito, P., Assunção, R., Ballance, S., Bohn, T., Bourlieu-Lacanal, C., Boutrou, R., Carriere, F., Clemente, A., Corredig, M., Dupont, D., Dufour, C., Edwards, C., Golding, M., Karakaya, S., Kirkhus, B., Feunteun, S. L., … Recio, I. (2019). INFOGEST static in vitro simulation of gastrointestinal food digestion. *Nature Protocols*, *14*(4), 991–1014. https://doi.org/10.1038/s41956-018-0119-1

Cavell, B. (1981). Gastric emptying in infants fed human milk or infant formula. *Acta Paediatrica Scandinavica*, *70*(5), 639–641.

Charton, E., Bourgeois, A., Bellanger, A., Gouar, Y., Dahirel, P., Cahu, A., Moughan, P., Montoya, C., Blat, S., Dupont, D., Deglaire, A., & Le Huërou-Luron, I. (2022). Infant nutrition affects the microbiota-gut-brain axis: Comparison of human milk vs. infant formula feeding in the piglet model. *Frontiers in Nutrition*, *9*. https://doi.org/10.3389/fnut.2022.976042

Church, F. C., Swaisgood, H. E., Porter, D. H., & Catignani, G. L. (1983). Spectrophotometric Assay Using o-Phthaldialdehyde for Determination of Proteolysis in Milk and Isolated Milk Proteins1. *Journal of Dairy Science*, *66*(6), 1219–1227. https://doi.org/10.3168/jds.S0022-0302(83)81926-2

Dalgalarrondo, M., Dufour, E., Chobert, J.-M., Bertrand-Harb, C., & Haertlé, T. (1995). Proteolysis of β-lactoglobulin and β-casein by pepsin in ethanolic media. *International Dairy Journal*, *5*(1), 1–14. https://doi.org/10.1016/0958-6946(94)P1595-5

de Oliveira, S., Deglaire, A., Ménard, O., Bellanger, A., Rousseau, F., Henry, G., Dirson, E., Carrière, F., Dupont, D., & Bourlieu, C. (2016). Holder pasteurization impacts the proteolysis, lipolysis and disintegration of human milk under in vitro dynamic term newborn digestion. *Food Research International*, *88*, 263–275. https://doi.org/10.1016/j.foodres.2015.11.022

Debry, G. (2001). *Lait, nutrition et santé*. Tec & Doc.

Dupont, D., Mandalari, G., Mollé, D., Jardin, J., Rolet-Répécaud, O., Duboz, G., Léonil, J., Mills, C. E. N., & Mackie, A. R. (2010). Food processing increases casein resistance to simulated infant digestion. *Molecular Nutrition & Food Research*, *54*(11), 1677–1689. https://doi.org/10.1002/mnfr.200900582

European Union. 2016. Commission directive 2016/127/EC of 25 september 2015 on infant formulas and follow-on formulas and completed regulation n° 609/2013 and amending directive 2006/141/EC. *European Commission*

Ewer, A. K., Durbin, G. M., Morgan, M. E., & Booth, I. W. (1994). Gastric emptying in preterm infants. *Archives of Disease in Childhood. Fetal and Neonatal Edition*, *71*(1), F24-27. https://doi.org/10.1136/fn.71.1.f24

Gallier, S., Vocking, K., Post, J. A., Van De Heijning, B., Acton, D., Van Der Beek, E. M., & Van Baalen, T. (2015). A novel infant milk formula concept: Mimicking the human milk fat globule structure. *Colloids and Surfaces. B, Biointerfaces*, *136*, 329–339. https://doi.org/10.1016/j.colsurfb.2015.09.024

Global UNICEF. (2022). *Global Databases: Infant and Young Child Feeding: Exclusive breastfeeding*. UNICEF.

Guyomarc'h, F., Queguiner, C., Law, A. J. R., Horne, D. S., & Dalgleish, D. G. (2003). Role of the soluble and micelle-bound heat-induced protein aggregates on network formation in acid skim milk gels. *Journal of Agricultural and Food Chemistry*, *51*(26), 7743–7750. https://doi.org/10.1021/jf030201x

Halabi, A. (2020a). *Formules infantiles modèles: Relation entre structures protéiques et comportement en digestion* [These de doctorat, Rennes, Agrocampus Ouest]. http://www.theses.fr/2020NSARB340

Halabi, A. (2020b). *Model infant milk formulas: Relationship between protein structures and digestive behaviour* [PhD Thesis, Agrocampus Ouest]. https://theses.hal.science/tel-03340179

Halabi, A., Croguennec, T., Bouhallab, S., Dupont, D., & Deglaire, A. (2020). Modification of protein structures by altering the whey protein profile and heat treatment affects in vitro static digestion of model infant milk formulas. *Food & Function*, *11*. https://doi.org/10.1039/D0FO01362E

Halabi, A., Croguennec, T., Ménard, O., Briard-Bion, V., Jardin, J., Le Gouar, Y., Hennetier, M., Bouhallab, S., Dupont, D., & Deglaire, A. (2022). Protein structure in model infant milk formulas impacts their kinetics of hydrolysis under in vitro dynamic digestion. *Food Hydrocolloids*, *126*, 107368. https://doi.org/10.1016/j.foodhyd.2021.107368

Hodgkinson, A. J., Wallace, O. A., Smolenski, G., & Prosser, C. G. (2019). Gastric digestion of cow and goat milk: Peptides derived from simulated conditions of infant digestion. *Food Chemistry*, *276*, 619–625. https://doi.org/10.1016/j.foodchem.2018.10.065

Huppertz, T., & Lambers, T. T. (2020). Influence of micellar calcium phosphate on in vitro gastric coagulation and digestion of milk proteins in infant formula model systems. *International Dairy Journal*, *107*, 104717. https://doi.org/10.1016/j.idairyj.2020.104717

International Organization for Standardization. (2014). *ISO 8968-1:2014—Milk and milk products—Determination of nitrogen content—Part 1: Kjeldahl principle and crude protein calculation*. https://www.iso.org/standard/61020.html

Joyce, A. M., Brodkorb, A., Kelly, A. L., & O'Mahony, J. A. (2017). Separation of the effects of denaturation and aggregation on whey-casein protein interactions during the manufacture of a model infant formula. *Dairy Science & Technology*, *96*(6), 787–806. https://doi.org/10.1007/s13594-016-0303-4

Kalab, M., Allan-Wojtas, P., & Phipps Todd, B. (1983). Development of microstructure in set-style nonfat yogurt-A Review. *Food Microstructure*, *2*, 51–66.

Langella, O., Valot, B., Balliau, T., Blein-Nicolas, M., Bonhomme, L., & Zivy, M. (2017). X!TandemPipeline: A Tool to Manage Sequence Redundancy for Protein Inference and Phosphosite Identification. *Journal of Proteome Research*, *16*(2), 494–503. https://doi.org/10.1021/acs.jproteome.6b00632

Le Huërou-Luron, I., Bouzerzour, K., Ferret-Bernard, S., Ménard, O., Le Normand, L., Perrier, C., Le Bourgot, C., Jardin, J., Bourlieu, C., Carton, T., Le Ruyet, P., Cuinet, I., Bonhomme, C., & Dupont, D. (2018). A mixture of milk and vegetable lipids in infant formula changes gut digestion, mucosal immunity and microbiota composition in neonatal piglets. *European Journal of Nutrition*, *57*(2), 463–476. https://doi.org/10.1007/s00394-016-1329-3

Le Roux, L., Ménard, O., Chacon, R., Dupont, D., Jeantet, R., Deglaire, A., & Nau, F. (2020). Are Faba Bean and Pea Proteins Potential Whey Protein Substitutes in Infant Formulas? An In Vitro Dynamic Digestion Approach. *Foods (Basel, Switzerland)*, *9*(3). https://doi.org/10.3390/foods9030362

Lee, G. O., McCormick, B. J., Seidman, J. C., Kosek, M. N., Haque, R., Olortegui, M. P., Lima, A. A., Bhutta, Z. A., Kang, G., Samie, A., Amour, C., Mason, C. J., Ahmed, T., Yori, P. P., Oliveira, D. B., Alam, D., Babji, S., Bessong, P., Mduma, E., … Caulfield, L. E. (2017). Infant Nutritional Status, Feeding Practices, Enteropathogen Exposure, Socioeconomic Status, and Illness Are Associated with Gut Barrier Function As Assessed by the Lactulose Mannitol Test in the MAL-ED Birth Cohort. *The American Journal of Tropical Medicine and Hygiene*, *97*(1), 281–290. https://doi.org/10.4269/ajtmh.16-0830

Lemaire, M. (2018). *The addition of dairy lipids and L. fermentum in infant formulas programs adult gut microbiota and physiology; study in a minipig model* [PhD Thesis, Rennes 1]. https://hal.inrae.fr/tel-02787777

Lemaire, M., Le Huërou-Luron, I., & Blat, S. (2018). Effects of infant formula composition on long-term metabolic health. *Journal of Developmental Origins of Health and Disease*, *9*(6), 573–589. https://doi.org/10.1017/S2040174417000964

Lönnerdal, B. (2016). Bioactive Proteins in Human Milk: Health, Nutrition, and Implications for Infant Formulas. *The Journal of Pediatrics*, *173 Suppl*, S4-9. https://doi.org/10.1016/j.jpeds.2016.02.070

Macierzanka, A., Sancho, A. I., Mills, E. N. C., Rigby, N. M., & Mackie, A. R. (2009). Emulsification alters simulated gastrointestinal proteolysis of β-casein and β-lactoglobulin. *Soft Matter*, *5*(3), 538–550. https://doi.org/10.1039/B811233A

Ménard, O., Picque, D., & Dupont, D. (2015). *The DIDGI®system*. 73–81. https://doi.org/10.1007/978-3-319-16104-4_8

Minkiewicz, P., Dziuba, J., Iwaniak, A., Dziuba, M., & Darewicz, M. (2008). BIOPEP Database and Other Programs for Processing Bioactive Peptide Sequences. *Journal of AOAC INTERNATIONAL*, *91*(4), 965–980. https://doi.org/10.1093/jaoac/91.4.965

Nebbia, S., Giribaldi, M., Cavallarin, L., Bertino, E., Coscia, A., Briard-Bion, V., Ossemond, J., Henry, G., Ménard, O., Dupont, D., & Deglaire, A. (2020). Differential impact of Holder and High Temperature Short Time pasteurization on the dynamic in vitro

digestion of human milk in a preterm newborn model. *Food Chemistry*, *328*, 127126. https://doi.org/10.1016/j.foodchem.2020.127126

Neelima, Sharma, R., Rajput, Y. S., & Mann, B. (2013). Chemical and functional properties of glycomacropeptide (GMP) and its role in the detection of cheese whey adulteration in milk: A review. *Dairy Science & Technology*, *93*(1), 21–43. https://doi.org/10.1007/s13594-012-0095-0

Nielsen, P. M., Petersen, D., & Dambmann, C. (2001). Improved Method for Determining Food Protein Degree of Hydrolysis. *Journal of Food Science*, *66*(5), 642–646. https://doi.org/10.1111/j.1365-2621.2001.tb04614.x

Oosting, A.-M., Kegler, D., Wopereis, H. J., Teller, I. C., van de Heijning, B. J. M., Verkade, H. J., & van der Beek, E. M. (2012). Size and phospholipid coating of lipid droplets in the diet of young mice modify body fat accumulation in adulthood. *Pediatric Research*, *72*(4), Article 4. https://doi.org/10.1038/pr.2012.101

Picariello, G., Miralles, B., Mamone, G., Sánchez-Rivera, L., Recio, I., Addeo, F., & Ferranti, P. (2015). Role of intestinal brush border peptidases in the simulated digestion of milk proteins. *Molecular Nutrition & Food Research*, *59*(5), 948–956. https://doi.org/10.1002/mnfr.201400856

Srinivasan, M., Singh, H., & Munro, P. A. (1996). Sodium Caseinate-Stabilized Emulsions: Factors Affecting Coverage and Composition of Surface Proteins. *Journal of Agricultural and Food Chemistry*, *44*(12), 3807–3811. https://doi.org/10.1021/jf960135h

Su, M.-Y., Broadhurst, M., Liu, C.-P., Gathercole, J., Cheng, W.-L., Qi, X.-Y., Clerens, S., Dyer, J. M., Day, L., & Haigh, B. (2017). Comparative analysis of human milk and infant formula derived peptides following in vitro digestion. *Food Chemistry*, *221*, 1895–1903. https://doi.org/10.1016/j.foodchem.2016.10.041

Swaisgood, H. E. (1992). Chemistry of the caseins. In *Advanced dairy chemistry-1: Proteins.* (pp. 63–110). Elsevier Applied Science. https://www.cabdirect.org/cabdirect/abstract/19930457634

Swaisgood, H. E. (2003). Chemistry of the Caseins. In P. F. Fox & P. L. H. McSweeney (Eds.), *Advanced Dairy Chemistry—1 Proteins: Part A / Part B* (pp. 139–201). Springer US. https://doi.org/10.1007/978-1-4419-8602-3_3

Thomä-Worringer, C., Sørensen, J., & López-Fandiño, R. (2006). Health effects and technological features of caseinomacropeptide. *International Dairy Journal*, *16*(11), 1324–1333. https://doi.org/10.1016/j.idairyj.2006.06.012

Van Den Driessche, M., Peeters, K., Marien, P., Ghoos, Y., Devlieger, H., & Veereman-Wauters, G. (1999). Gastric emptying in formula-fed and breast-fed infants measured with the 13C-octanoic acid breath test. *Journal of Pediatric Gastroenterology and Nutrition*, *29*(1), 46–51. https://doi.org/10.1097/00005176-199907000-00013

van Lieshout, G. A., Lambers, T. T., Bragt, M. C., & Hettinga, K. A. (2019). How processing may affect milk protein digestion and overall physiological outcomes: A systematic review. *Critical Reviews in Food Science and Nutrition*, 1–24. https://doi.org/10.1080/10408398.2019.1646703

Wada, Y., & Lönnerdal, B. (2014). Bioactive peptides derived from human milk proteins—Mechanisms of action. *The Journal of Nutritional Biochemistry*, *25*(5), 503–514. https://doi.org/10.1016/j.jnutbio.2013.10.012

Wada, Y., Phinney, B. S., Weber, D., & Lönnerdal, B. (2017). In vivo digestomics of milk proteins in human milk and infant formula using a suckling rat pup model. *Peptides*, *88*, 18–31. https://doi.org/10.1016/j.peptides.2016.11.012

Wang, X., Ye, A., Lin, Q., Han, J., & Singh, H. (2018). Gastric digestion of milk protein ingredients: Study using an in vitro dynamic model. *Journal of Dairy Science*, *101*(8), 6842–6852. https://doi.org/10.3168/jds.2017-14284

Ye, A., & Singh, H. (2001). Interfacial composition and stability of sodium caseinate emulsions as influenced by calcium ions. *Food Hydrocolloids*, *15*(2), 195–207. https://doi.org/10.1016/S0268-005X(00)00065-5

Yu, X., Leconte, N., Méjean, S., Garric, G., Even, S., Henry, G., Tessier, F. J., Howsam, M., Croguennec, T., Gésan-Guiziou, G., Dupont, D., Jeantet, R., & Deglaire, A. (2021). Semi-industrial production of a minimally processed infant formula powder using membrane filtration. *Journal of Dairy Science*, *104*(5), 5265–5278. https://doi.org/10.3168/jds.2020-19529

Tables:

Table 1: Characteristics of the whey protein ingredients used in the IFs

Item	*Units*	Demineralized whey	Demineralized whey protein concentrate	Demineralized whey
Lactoserum origin		Cheese whey	Cheese whey	Ideal whey
Crude protein[1]	*g / kg of powder*	115.5 ± 0.1	777.2 ± 4.7	118.4 ± 0.3
True protein[1]	*% of crude protein*	85.6 ± 0.0	94.0 ± 0.6	92.3 ± 0.0
Non-protein nitrogen[1]	*% of crude protein*	14.4 ± 0.1	6.1 ± 0.0	7.7 ± 0.0
β-lactoglobulin (BLG)[2]	*% of protein nitrogen*	59	53	64
α-lactalbumin (ALA)[2]	*% of protein nitrogen*	12	10	14
Glycomacropeptide		Presence	Presence	Absence
Tryptophan[3]	*% of crude protein*	1.7	1.7	2.2
BLG denaturation[4]	*% of total BLG*	22	0	1.7
ALA denaturation[4]	*% of total ALA*	59	0	22
Blocked Lysine[5]	*% of total lysine*	19	13	14
Corresponding IF		A	B	C and D

Determined by Kjeldahl method with a N-to-protein factor conversion of 6.38; [2] Determined by RP-HPLC; [3] Externalized measurements made by HPLC; [4] Calculated by the ratio of native BLG or ALA (NATIVE-PAGE) and total BLG or ALA (SDS-PAGE); [5] Determined by a fast and non-destructive fluorescence technique developed by SODIAAL (Eurosérum, Port-sur-Saône, France) using a model developed on Amaltheys (Spectralys Innovation, Asnières-sur-Seine, France).

Table 2: Biochemical composition (± SD) of the 4 powdered IFs, following the European regulation (EU, 2016/127)

	Per kg of powder				
Item	Unit	IF A	IF B	IF C	IF D
Crude protein[1]	g	114.1 ± 0.6	104.0 ± 0.1	115.5 ± 0.1	113.0 ± 0.1
True protein[1]	g	101.7 ± 0.4	95.6 ± 0.1	107.6 ± 0.1	105.9 ± 0.1
Non-protein nitrogen[1]	g	12.4 ± 0.2	8.4 ± 0.01	7.9 ± 0.03	7.1 ± 0.01
Casein:WP[2]	%	40:60	40:60	40:60	40:60
Denaturation[3]	% of total WPs	44.3 ± 0.01	35.9 ± 0.2	30.9 ± 0.2	29.3 ± 0.1
Tryptophan[4]	g	1.53 ± 0.18	1.46 ± 0.11	1.89 ± 0.01	1.75 ± 0.04
Lipids[5]	g	284 ± 0.5	260 ± 0.4	264 ± 0.3	264 ± 0.3
Lactose[2]	g	567	571	573	573
Ash[2]	g	2,5	2,5	2,5	2,5
Sodium[2]	mg	225	225	225	225
Potassium[2]	mg	568	569	567	567
Calcium[2]	mg	369	370	370	370
Phosphorus[2]	mg	278	277	279	279
Iron[2]	mg	4	4	4	4
Zinc[2]	mg	4	4	4	4

Magnesium[2]	mg	54	54	54	55
Chloride[2]	mg	542	452	452	452
Iodine[2]	µg	114	114	115	115
Copper[2]	µg	412	412	412	412
Manganese[2]	µg	184	184	185	185
Selenium[2]	µg	33	32	33	33
Energy[2]	kcal	515	516	514	514
	kJ	2155	2157	2149	2151

[1] Determined by Kjeldahl method with a N-to-protein conversion factor of 6.38; [2] Expected according to the formulation; [3] Calculated using Equation.1 described in 2.4.1; [4] Determined by the method described in Charton et al., 2022; [5] Determined by Teicher method

Table 3: Modal diameter of the main particles peak in undigested (G0) and digested (G40, G80 and G120) IFs (A/B/C/D) at digestive pH (6.8, 5.6, 4.8 and 4.2) determined by laser light scattering.

pH	IF	Mode 0 of undigested IF (µm)	Mode 0 of digested IFs (µm)
6.8 (G0)	A	0.66 ± 0.0	/
	B	0.62 ± 0.0	/
	C	0.63 ± 0.0	/
	D	0.60 ± 0.0	/
5.6 (G40)	A	0.65 ± 0.0	17.4 ± 2.7
	B	0.61 ± 0.0	20.2 ± 0.7

	C	0.61 ± 0.0	13.2 ± 2.4
	D	0.62 ± 0.0	9.2 ± 1.1
4.8 (G80)	A	99.2 ± 11.9	37.0 ± 3.1
	B	127.9 ± 11.2	30.4 ± 3.8
	C	100.2 ± 6.6	29.2 ± 0.1
	D	95.5 ± 5.5	26.5 ± 3.6
4.2 (G120)	A	91.6 ± 6.2	34.3 ± 0.6
	B	102.2 ± 8.2	25.0 ± 1.0
	C	99.0 ± 2.6	26.2 ± 0.2
	D	80.4 ± 3.9	24.2 ± 2.6

Figure captions:

Figure 1: Processing route of the protein ingredients used in the IFs

Figure 2: Structure of the undigested IFs determined by (A) particle size distribution, (B) confocal laser scanning microscopy and transmission electronic microscopy and (C) flow-field flow fractionation; (D) schematical representation of IF structures

(A) Each measurement was performed in triplicate on undigested IFs at pH 6.7. (B) Images were made on two independent samples. Confocal images were observed at a magnification of x 1.8. Proteins were coloured in green (FrastGreen®) and lipids in red (RedNile®). Scale bar: 5 µm. TEM images were observed at a magnification of x 20 000. Microstructures of interest described in the article were circled in red. In IF-D, abnormal large green particles are insoluble micronic particles. (C) Solid lines represent concentrations. Dotted lines represent gyration radius (Rg). Each measurement was performed in duplicate. No data could be obtained for IF-D because of technical difficulties.

Figure 3: Evolution of IF structure during the gastric phase of in vitro digestion, determined by (A) particle size distribution, (B) confocal laser scanning microscopy

(A) Data represent means of three independent digestion experiment (n = 3), with each measurement performed in triplicate. G40 = 40 min of gastric phase; G80 = 80 min of gastric phase; G120 = 120 min of gastric phase. Undigested sample corresponds to the IF adjusted to the pH observed at the different stages of gastric digestion. (B) Images were from two independent samples. Confocal images were observed at a magnification of x 1.8. Proteins were coloured in green (FastGreen®) and lipids in red (RedNile®). Scale bar: 5 µm.

Figure 4: Kinetics of proteolysis of the IFs during gastro-intestinal digestion, as evaluated by (A) o-phtalaldehyde assay, (B) SDS-PAGE for the proportion of residual intact proteins in the gastric phase and (C) amino acid bioaccesibility.

Data represent means ± SD (n = 3) except for residual intact proteins of IF-C where n = 2 due to a non-representative sampling. Data from undigested IFs were not included in the statistical analysis. Statistically significant factors were references with $p < 0.001$ (***), $p < 0.01$ (**), $p < 0.05$ (*) and $p > 0.05$ (NS). Different subscript letters represent significant differences among treatments within IFs ($p < 0.05$). During whole digestion, as the digestion time reflected hydrolysis kinetic, a significant effect on residual intact proteins was observed for this variable (p-value < 0.001). Abbreviations: IF for infant formula; A, B, C and D for IF-A, IF-B, IF-C and IF-D; Met for methionine; Phe for phenylalanine; Ile for isoleucine.

Figure 5: (A) Clusters of parent protein (on left) and (B) heatmap abundances as classified by hierarchical classification (on right) present in gastric (G80, G180) and intestinal (I20, I40, I80, I180) digesta of the 4 IFs

Each peptide abundance was log10-transformed and divided by its maximum abundance so that to have a maximum abundance value of 1. Peptides were identified using a homemade protein database composed of major bovine milk proteins (131 proteins). (A) Clusters were made with all the identified peptides released during the in vitro dynamic gastrointestinal digestion of the IFs. (B) Light yellow indicates low abundance graduating to dark blue for high abundance of peptides identified. A, B, C and D for IF-A, IF-B, IF-C and IF-D; G80: 80 min of gastric phase, G180: 180 min of gastric phase, I20: 20 min of intestinal phase, I40: 40 min of intestinal phase, I80: 80 min of intestinal phase, I180 : 180 min of intestinal phase; β-cas: β-casein; α_{s1}-cas: α_{s1}-casein; κ-cas: κ-casein; α_{s2}-cas: α_{s2}-casein; GLC1: glycam 1; LF: lactoferrin; BLG: β-lactoglobulin; ALA: α-lactalbumin; BSA: bovine serum albumin; OSTP: osteopontin.

Figure 6: Heatmap of the abundance of bioactive peptides identified in (A) gastric phase and (B) intestinal phase during *in vitro* dynamic digestion, with their peptide sequence and activity.

Peptide abundances were log10-transformed followed by setting a maximal abundance to 1. Blue colour indicates low abundance graduating to red colour for high abundance of identified peptide. Bioactive peptides have been identified using BIOPEP database. Abbreviations: A, B, C and D for IF-A, IF-B, IF-C and IF-D; G80: 80 min of gastric phase, G180: 180 min of gastric phase, I20: 20 min of intestinal phase, I40: 40 min of intestinal phase, I80: 80 min of intestinal phase, I180: 180 min of intestinal phase

Authors statement :

Lucile Chauvet: Investigation, Writting – Original Draft; Olivia Ménard, Yann Le Gouar, Gwénaële Henry, Julien Jardin, Marie Hennetier: Investigation; Thomas Croguennec, Marieke Van Audenhaege, Didier Dupont, Marion Lemaire, Isabelle Le Huërou-Luron, Amélie Deglaire: Supervision, Writting – Review & Editing.

Highlights:

- Whey proteins (WPs) denaturation impacts the microstructure of infant formula (IF)
- Casein supramolecular organisation impacts the microstructure of IF
- Proteolysis is favoured during *in vitro* dynamic digestion when WPs are more denatured
- Modification of casein organisation in IFs impacts their peptide release kinetics

Conflict of interests:

This work was supported by SODIAAL International, a French dairy cooperative, as a CIFRE (Agreement of Training through Research) PhD. Lucile CHAUVET, Marieke Van Audenhaege and Marion Lemaire are employed by SODIAAL International. Other authors declare no conflict of interests.

Graphical Abstract

Click here to access/download;Graphical Abstract;Graphical_abstract_CHAUVET_Lucile.tif

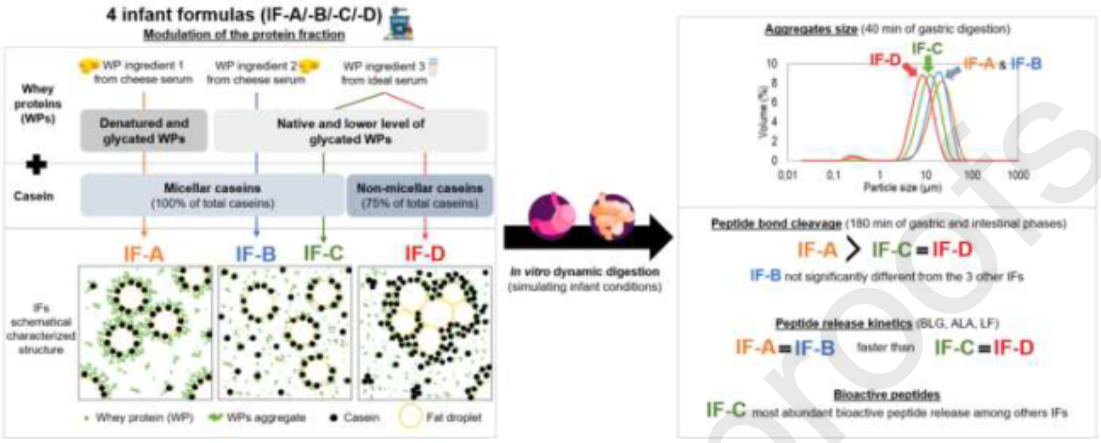

Figure 1

Click here to access/download;Figure;FIG1.tif

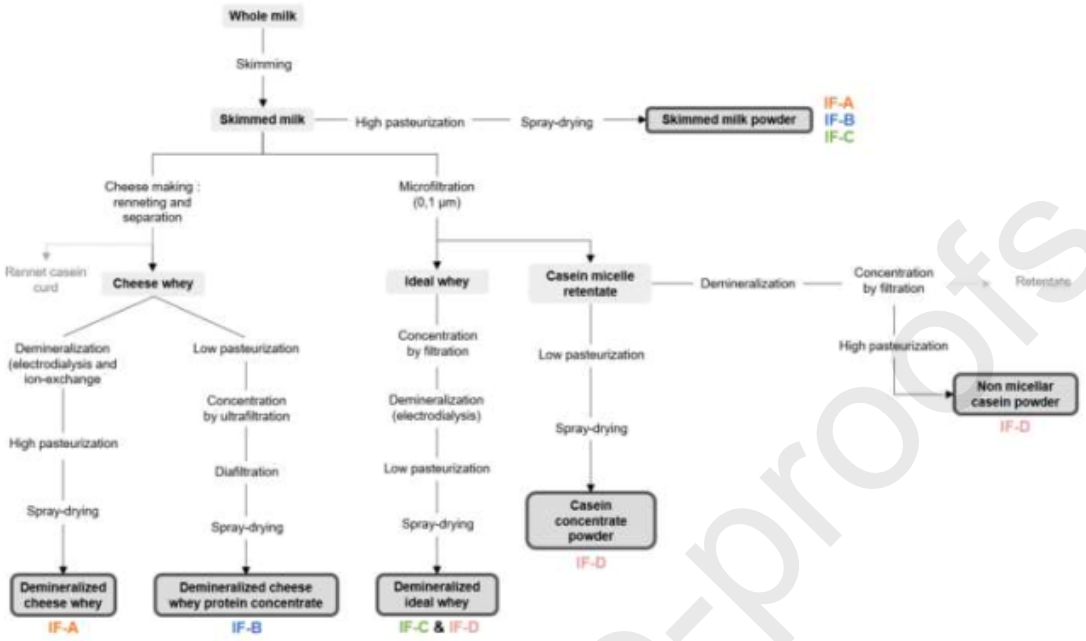

Figure 2

Click here to access/download;Figure;FIG2.tif

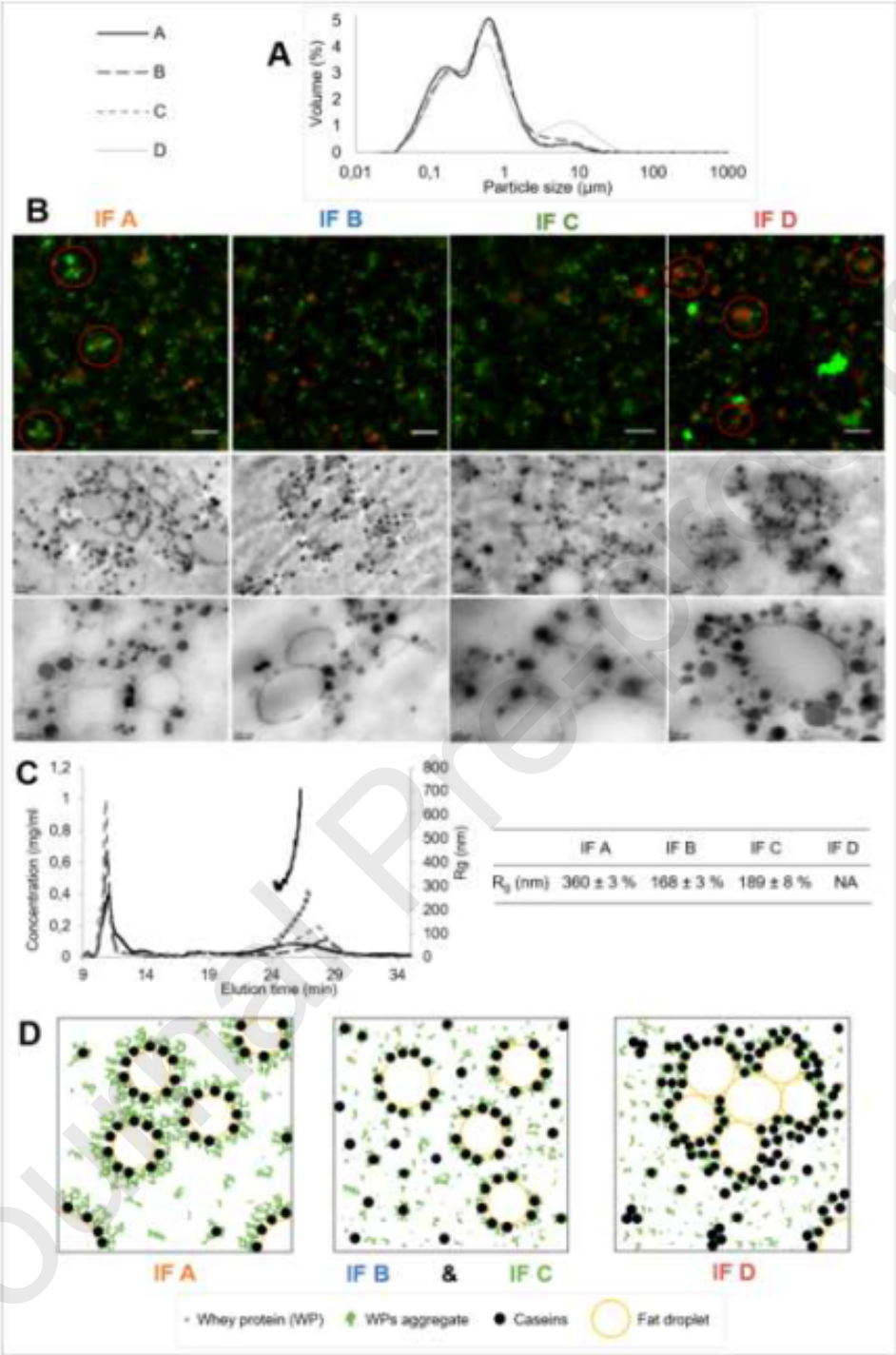

Figure 3

Click here to access/download;Figure;FIG3.tif

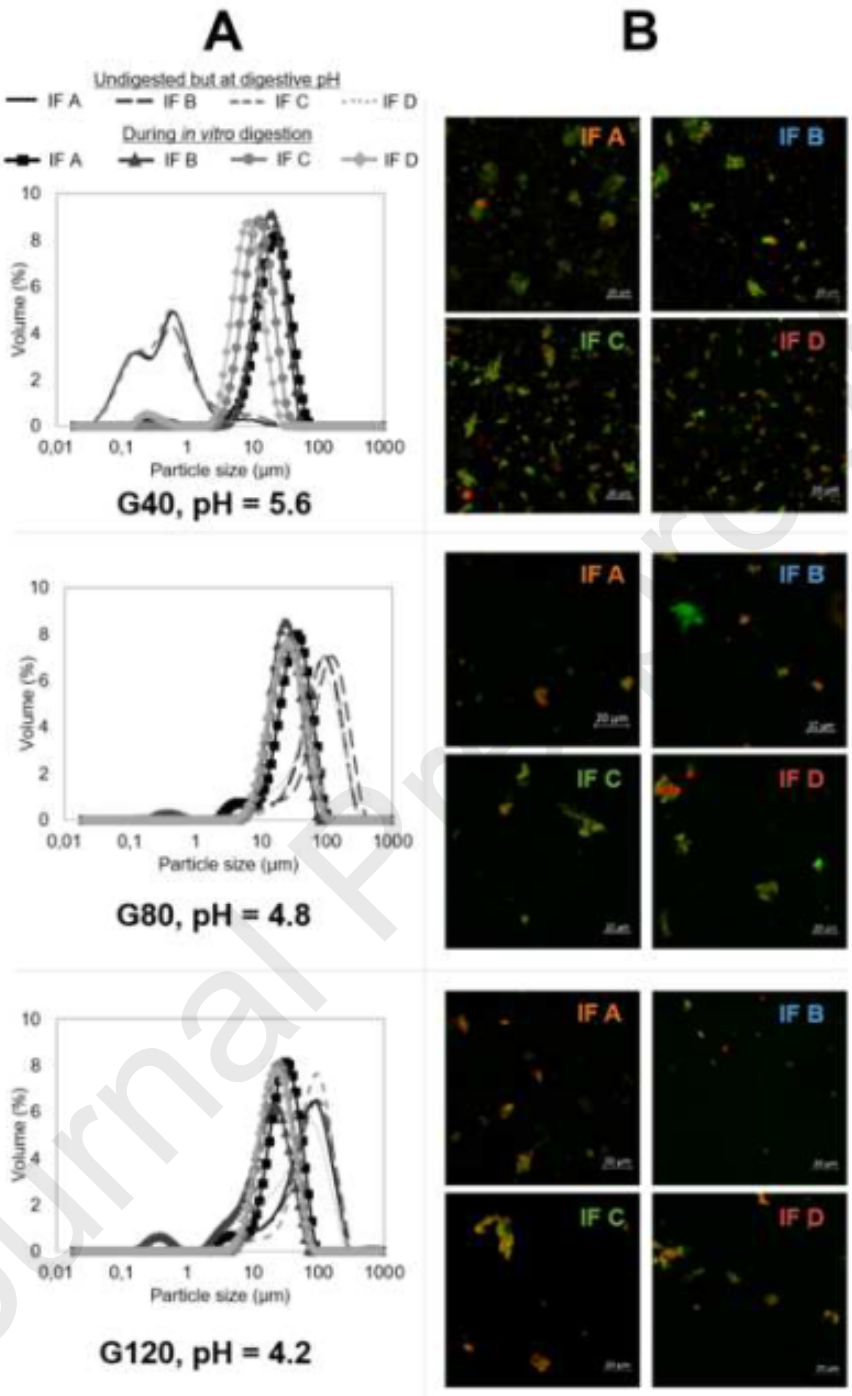

Figure 4

Click here to access/download;Figure;FIG4.tif

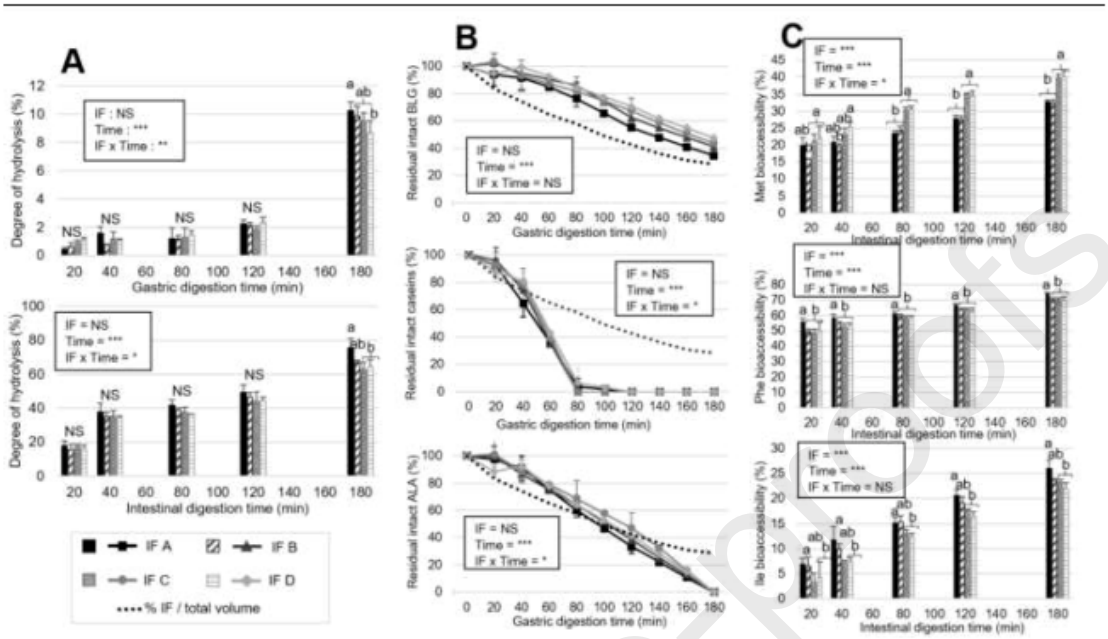

Figure 5

Click here to access/download;Figure;FIG5.tif

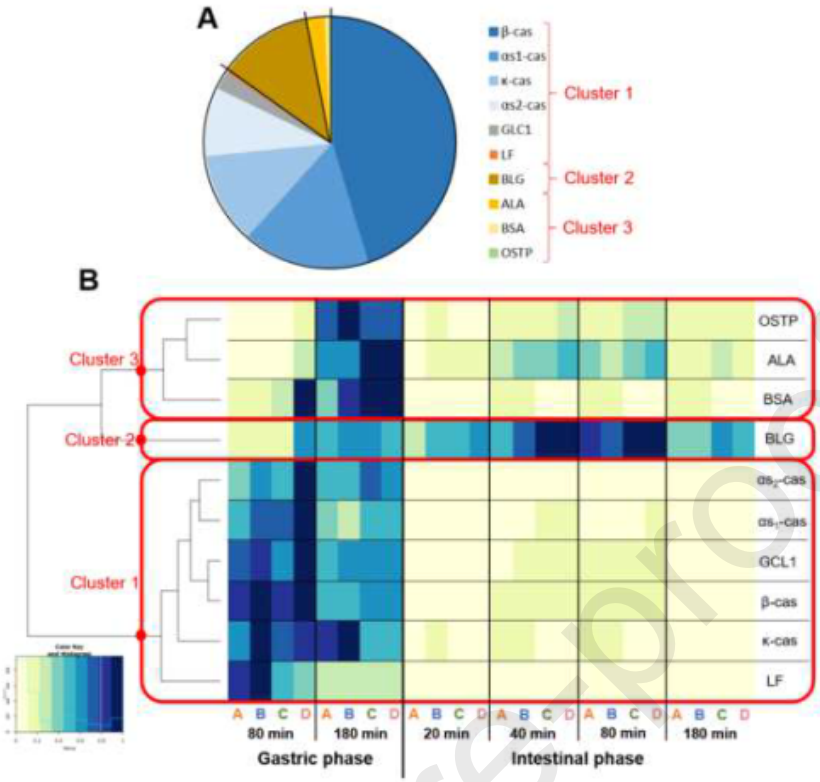

Figure 6

Click here to access/download;Figure;FIG6.tif